Chemical and Thin-Film Strategies for New Transparent Conducting Oxides

A.J. Freeman, K.R. Poeppelmeier, T.O. Mason, R.P.H. Chang, and T.J. Marks

Introduction

Transparent conducting oxides (TCOs) have been known and employed technologically for more than 50 years, primarily in the form of doped single-cation oxides such as In_2O_3 and SnO_2. Beginning in the 1990s, however, multi-cation oxide TCOs began to be developed in Japan (see the article by Minami in this issue and the references therein) and at the former Bell Laboratories.[1,2] Since then, new TCO phases are being reported with increasing frequency as technological interest in this area heightens. At the same time, our fundamental understanding of the chemical and structural origins of transparent conductivity continues to expand and promises a pathway to dramatically improved materials for a host of applications. This article describes a collaborative, multi-investigator bulk and thin-film research effort at Northwestern University aimed at the synthesis, characterization, and enhanced understanding of multi-cation (compound and solid-solution) TCOs, and provides a brief account of what we are discovering about this important class of materials. In particular, our research to date indicates that

- Many new and novel compound and solid-solution bulk TCOs remain to be discovered within TCO "phase space."
- Extended solid-solution phases afford tailorable TCO properties, such as optical gap and/or work function, in addition to electronic conductivity.
- The most promising multi-cation TCO materials share common chemical and structural features and possess similar carrier-generation mechanisms.
- Metastable TCO phases and solution ranges not available in bulk form can be obtained as thin films.
- In many instances, these complex new materials have properties comparable or superior to those of conventional TCOs, and their characterization should therefore be highly instructive.

Combinatorics and New Bulk Phases

We begin by considering oxides of five closely grouped d^{10} cations known to be constituents of transparent conductors (Zn^{2+}, Cd^{2+}, In^{3+}, Ga^{3+}, and Sn^{4+}). Four of these form TCOs as single-cation oxides (ZnO, CdO, In_2O_3, and SnO_2) when appropriately doped, whereas Ga_2O_3 is a wide-bandgap insulator. There are 10 binary, 10 ternary, five quaternary, and one quintinary, or a total of 26, combinations of these five oxides, most of which have not been fully explored insofar as stable phases, solid-solution ranges, and novel TCO phases are concerned.

The ternaries in this "phase space" can be further divided into four categories based upon cation charge, namely, divalent (Zn and Cd), trivalent (In and Ga), and tetravalent (Sn), including (2-2-3), (2-2-4), (3-3-4), and (2-3-4) systems. Figure 1 displays the (2-3-3), the (3-3-4), and the two (2-3-4) systems highlighting TCO phases discovered and/or investigated at Northwestern. Non-TCO phases also exist, but have been omitted from the diagrams for clarity; complete or nearly complete subsolidus phase diagrams have been elucidated and are available elsewhere.[3–6] The chemical formulae and solid-solution ranges of these phases are detailed in Table I. Note that the T-phase (T = tetrag-

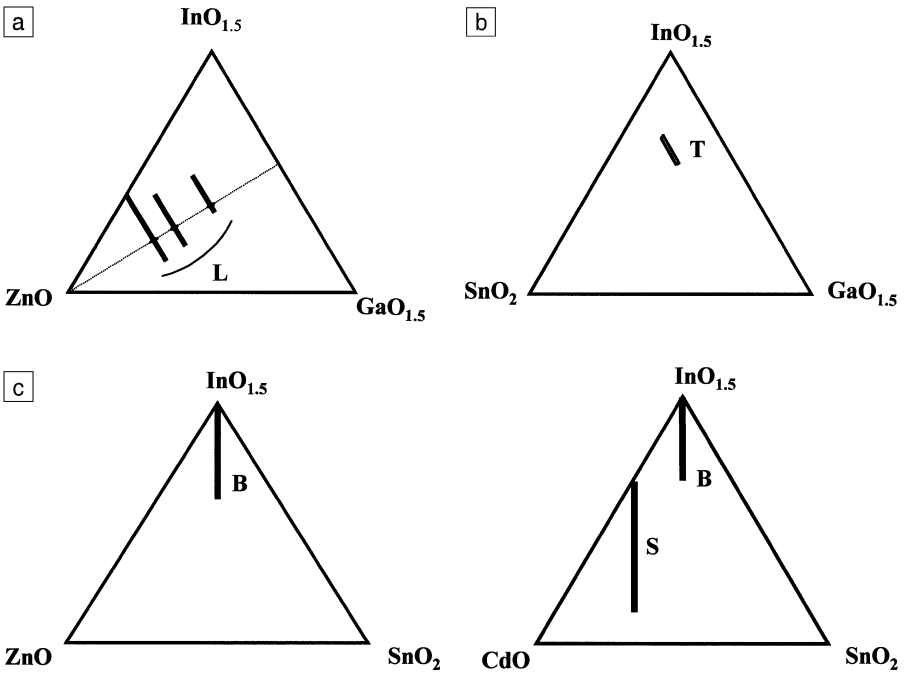

Figure 1. Transparent conducting oxide (TCO) phase space explored at Northwestern University, including (a) a 2-3-3 system, (b) a 3-3-4 system, and (c) two 2-3-4 systems, where the numbers represent cation charges.

Table I: Chemical Formulae, Crystal Structures, and Solution Ranges of TCO Phases.

System	Phase	Formula
Zn-In-Ga	Layered intergrowths	$In_{1-x}Ga_{1+x}O_3(ZnO)_k$: $k = 1$ ($-0.34 < x < 0.06$) $k = 2$ ($-0.54 < x < 0.3$) $k = 3$ ($-1 < x < 0.42$)
Ga-In-Sn	T-phase	$Ga_{3-x}In_{5+x}Sn_2O_{16}$ ($0.3 < x < 1.6$)
Zn-In-Sn	Bixbyite	$In_{2-2x}Sn_xZn_xO_3$ ($0 < x < 0.4$)
Cd-In-Sn	Spinel	$Cd_{1+x}In_{2-2x}Sn_xO_4$ ($0 < x < 0.75$)
Cd-In-Sn	Bixbyite	$In_{2-2x}Sn_xCd_xO_3$ ($0 < x < 0.34$)

onal) in the (Ga-In-Sn)-O system and the extended bixbyite (B) and spinel (S) solid-solution ranges in (Zn-In-Sn)-O and (Cd-In-Sn)-O were unknown prior to our work. Furthermore, the T-phase is the first true ternary TCO with a previously unknown crystal structure[7,8] and has no known counterpart in the existing binary or ternary systems. Its existence suggests that we are only just beginning to explore TCO phase space for novel materials.

Chemical and Structural Insights

The lines in Figure 1 represent the ranges of composition available in the various TCO phases, as detailed in Table I. In every instance, we can understand them in terms of essentially "isovalent" substitutions. For example, in the (3-3-4) systems, Ga^{3+} substitutes for In^{3+} over broad ranges of composition. The "L" (layered) compounds in the (Zn-In-Ga)-O system, originally characterized in Japan,[9] are identical in structure to the homologous series, $(ZnO)_kIn_2O_3$, in the bounding (Zn-In)-O binary.[5,10,11] It is interesting to note that the $k = 1$ and $k = 2$ members, which do *not* readily form in the binary, are stable with the Ga present. In fact, we have suggested that the "parent" compounds for these phases are in reality the 50:50 In:Ga compositions, that is, $(ZnO)_k(InGaO_3)$, which would make these phases essentially "ternary" in nature.[5] In both the "L" and "T" phases, the latter referring to the ternary (Ga-In-Sn)-O compound already described, the isovalent substitution of Ga^{3+} for In^{3+} serves to gradually modify the TCO properties, with optical gap widening and electrical conductivity diminishing. This is most likely due to the dilution of In on octahedral sites, which we believe to be essential for good conductivity.

Isovalent substitution also takes place in the (2-3-4) systems of Figure 1. In both the "B" (bixbyite) and "S" (spinel) phases, the co-substitution of 2+ (Zn or Cd) and 4+ (Sn) species for two 3+ (In) species provides for self-compensation. For instance, in Kröger-Vink (K-V) notation,

$$CdO + SnO_2 + 2\,In_{In}^{x} \Rightarrow Cd_{In}'' + Sn_{In}^{\bullet\bullet} + In_2O_3. \quad (1)$$

As a reminder, in K-V notation, the capital letter stands for the defect or ionic species, the subscript stands for the site, and the superscript stands for effective charge, whether negative ($'$) or positive ($^{\bullet}$). The extensive co-substitution of Zn^{2+}/Sn^{4+} or Cd^{2+}/Sn^{4+} for In^{3+} in bixbyite (34–40% of the In ions can be replaced) is particularly noteworthy, since the solubility of each constituent by itself in In_2O_3 is either much smaller (Sn) or essentially negligible (Zn, Cd). As in the (3-3-4) solid solutions, TCO properties change gradually across the solid-solution ranges. Zn/Sn co-substitution tends to decrease conductivity in bixbyite,[12] whereas Cd/Sn co-substitution tends to increase conductivity in both bixbyite and spinel materials.[6,13]

One important ramification of the extended TCO phase solid-solution ranges in the (2-3-4) and (3-3-4) systems is the opportunity for compositionally tailored properties, such as "bandgap engineering," as is common practice with compound semiconductors, and/or "work function engineering." The work function is an especially important parameter for electrode matching with semiconductors in photovoltaic and light-emitting diode applications. It should also be noted that property changes are even more pronounced as the interlayer spacing k is increased in the homologous series compounds, $(ZnO)_k(InGaO_3)$.[3]

After characterizing the electrical properties of $CdSnO_3$, orthorhombic Cd_2SnO_4, In_2TeO_6, and $CdIn_2O_4$, Shannon et al.[14] noted a correlation between edge-sharing octahedral chains of Cd^{+2}, In^{+3}, and Sn^{+4} and transparent conduction. Our work to date on the ternary systems of Figure 1 similarly suggests that optimum TCOs involve In or a combination of Cd with either In or Sn in octahedral coordination. In fact, all the complex (ternary compound or solid-solution) TCOs in Figure 1 possess cations in octahedral coordination, as do most single-oxide TCOs, including CdO, In_2O_3, and SnO_2. ZnO is the lone exception, with a continuous array of cations in tetrahedral coordination.

Indium oxide (cubic bixbyite structure), when Sn-doped to form indium tin oxide (ITO), is the most extensively used TCO because of its good conductivity, transparency, and other properties. When co-doped according to Equation 1, the conductivity increases with Cd/Sn substitution, but decreases with Zn/Sn substitution.[6,12] Both sites in bixbyite are octahedrally coordinated. The Zn is therefore not as effective in octahedral site co-substitution with Sn as is Cd in enhancing TCO behavior. We also have found the Zn_2SnO_4 spinel (not shown in Figure 1) to be a relatively poor conductor.[15] The cation distribution is most likely "inverse" ($(Zn(SnZn)O_4$), given the propensity of Sn^{4+} for octahedral coordination.[15] The poor TCO behavior of Zn_2SnO_4 suggests that octahedral Sn (without Cd present), Zn in either site, and Zn/Sn in octahedral site combination are not nearly as effective as the other cations or combinations in producing TCO behavior. However, upon In substitution for Zn/Sn (the reverse of Equation 1), the electrical conductivity of Zn_2SnO_4 increases significantly.

The spinel solid solution in Figure 1 offers another case in point. $CdIn_2O_4$, along the (Cd-In)-O binary, is a good TCO, owing to In or possibly a combination of Cd and In on octahedral sites.[13] With Cd/Sn co-substitution for In (Equation 1), however, the conductivity is significantly enhanced. Cubic Cd_2SnO_4, not stable in bulk form but readily obtained in films, exhibits high electronic mobility and good transparency.[16] This material is known to have an inverse distribution, $Cd(CdSn)O_4$.[17,18] These results suggest that the enhancement in electronic conductivity with Cd_2SnO_4 content in the $CdIn_2O_4$-Cd_2SnO_4 solution is attributable to the replacement of octahedral In by octahedral Cd/Sn (Equation 1), just as in the case of Cd/Sn co-substituted bixbyite.

The "L" phases in the (Zn-Ga-In)-O system consist of In-rich layers with In in octahedral coordination interleaved with Zn-rich layers (tetrahedral coordination).[11] We have demonstrated that the conductivity falls continuously as the number of (ZnO) layers increases.[5,10] Again, this suggests that the conductivity derives primarily from the octahedrally coordinated In layers.

Carrier-Generation Mechanisms

Both spinel and bixbyite phases exhibit important self-compensating and carrier-generation mechanisms, as detailed in Table II. We have already alluded to the distribution of cations between tetrahedral and octahedral sites in the spinel phase. In K-V notation, the thermal redistribution of cations in Cd_2SnO_4 can be represented as:

$$Cd_{Cd}^{x} + Sn_{Sn}^{x} \Longleftrightarrow Cd_{Sn}'' + Sn_{Cd}^{\bullet\bullet}, \quad (2)$$

which is clearly self-compensating, that is, electroneutrality is preserved. This reaction is important for two reasons. First, cation redistribution can change the composition of the tetrahedral—and more important, the octahedral—sites in the TCO. Second, it produces anti-site defects, which if present in unequal numbers, can influence the carrier concentration. For example, if $[Sn_{Cd}^{\bullet\bullet}] > [Cd_{Sn}'']$, the excess $Sn_{Cd}^{\bullet\bullet}$ species will serve as electron donors.

In In_2O_3 (cubic bixbyite structure), Sn doping is believed to take place preferentially by another self-compensating reaction,[19,20]

$$2In_{In}^{x} + 2SnO_2 \Rightarrow (2Sn_{In}^{\bullet}O_i'')^{x} + In_2O_3, \quad (3)$$

with the formation of neutral 2:1 $Sn:O_i$ associates. We have just obtained the first direct confirmation of the existence of oxygen interstitials in ITO at nearly a 2:1 $Sn:O_i$ ratio (unreduced material) by Rietveld analysis of neutron-diffraction data.[21] We believe these defects are essential for the Sn doping of ITO. For example, the T-phase in the (Ga-In-Sn)-O system possesses one, but not both, of the octahedral sites that exist in bixbyite (see Figure 2).[8] In contrast to ITO, we cannot detect excess Sn solubility (within a 1% detectability limit) in the T-phase. One possible explanation is that both sites are required for the 2:1 clusters to be stable in detectable concentrations.

Several carrier-generation mechanisms are possible in ITO, as given in Table II. First, direct doping with Sn donors is possible. Evidence suggests, however, that most Sn is incorporated as neutral species (associates).[19,20] The other mechanisms rely on reduction to activate the donor species. The dominant mechanism appears to be the removal of oxygen interstitials according to:

$$(2Sn_{In}^{\bullet}O_i'')^{x} \Longleftrightarrow 2Sn_{In}^{\bullet} + 1/2O_2(g) + 2e'. \quad (4)$$

Once all donor species are "activated," the carrier content changes little with further reduction until the onset of significant oxygen-vacancy formation under highly reducing conditions:

$$O_O^{x} \Longleftrightarrow 1/2O_2(g) + V_O^{\bullet\bullet} + 2e'. \quad (5)$$

Oxygen vacancies can also serve as electron donors. Three distinct regimes (i.e., electroneutrality approximations that govern the defect chemistry) have therefore been observed in ITO and the related T-phase: associate-dominated at high oxygen partial pressure p_{O_2}, vacancy-dominated at low p_{O_2}, and free-donor-dominated (fully reduced associates) at intermediate p_{O_2}.[3,19]

Our knowledge of carrier-generation mechanisms in the (Cd-In-Sn)-O spinels is on less sure footing. One possible mechanism involves anti-site defects (Equation 2). For example, if there are more $Sn_{Cd}^{\bullet\bullet}$ than Cd_{Sn}'' (e.g., through the preferential evaporation of Cd), the excess $Sn_{Cd}^{\bullet\bullet}$ can serve as donors. We know that anti-site defects are common in such spinels, owing to the cation redistribution reaction of Equation 2. Another possibility is the formation of interstitial cation species, which is also quite common in spinels.[22] It is well known that annealing Cd_2SnO_4 in a CdS-rich environment greatly enhances the electronic conductivity.[16,23] This is presumably due to the formation of cadmium interstitials, $Cd_i^{\bullet\bullet}$. Finally, the formation of oxygen vacancies (Equation 5) can also contribute to carrier production.

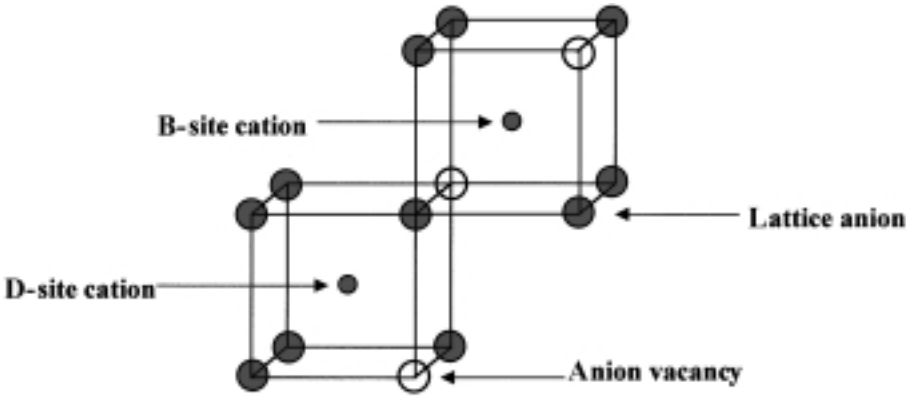

Figure 2. Nonequivalent cation sites in the bixbyite structure.

Band Structure

Our understanding of how doping and carrier generation alters the band structure of transparent conductors has been greatly aided by investigations made using highly precise first-principles band-structure techniques [full-potential linearized augmented plane wave (FLAPW) methods and full-potential linear muffin-tin orbital (FLMTO) methods].[24] Figure 3 displays the calculated band structures of undoped and Sn-doped In_2O_3, illustrating the essential features of transparent conductivity, that is, a highly dispersed single *s* band at the bottom of the conduction band, which

Table II: TCO Defect Models.

System	Self-Compensating Mechanism	Donor Generation
$In_2O_3:Sn$ (ITO)	$2In_{In}^{x} + 2SnO_2 \rightarrow (2Sn_{In}^{\bullet}O_i'')^{x} + In_2O_3$	$2In_{In}^{x} + 2SnO_2 \rightarrow 2Sn_{In}^{\bullet} + 2e' + In_2O_3 + 1/2O_2(g)$ $(2Sn_{In}^{\bullet}O_i'') \rightarrow 2Sn_{In}^{\bullet} + 2e' + 1/2O_2(g)$ $O_O^{x} \rightarrow 1/2O_2(g) + V_O^{\bullet\bullet} + 2e'$
Cd_2SnO_4	$Cd_{Cd}^{x} + Sn_{Sn}^{x} \rightarrow Cd_{Sn}'' + Sn_{Cd}^{\bullet\bullet}$	$[Sn_{Cd}^{\bullet\bullet}] > [Cd_{Sn}'']$ $Cd(g) \rightarrow Cd_i^{\bullet\bullet} + 2e'$ $O_O^{x} \rightarrow 1/2O_2(g) + V_O^{\bullet\bullet} + 2e'$

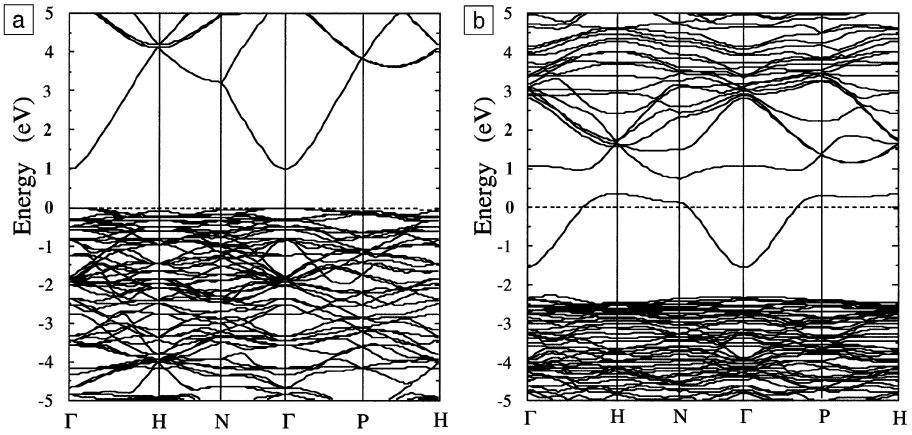

Figure 3. Electronic band structures calculated for (a) undoped and (b) Sn-doped indium oxide.[24]

explains the well-known Burstein-Moss (B-M) shift (i.e., increase in bandgap with carrier doping) and the presence of bandgaps (including those induced by the doping hybridization gap in the conduction band), which provide low-intensity absorption in the visible range. The high dispersion and *s*-type character of this band also explain the high conductivity due to the high mobility of these states and result in a rather uniform distribution of their electron charge density and hence their relatively low scattering. The opening of the second gap effectively lowers the plasma frequency ω_p, since it is roughly proportional to the largest energy of the intraband transition.

On the basis of these calculated band structures[24] and those recently obtained for CdO,[25] we formulated conditions for transparent conducting behavior: (1) a highly dispersed single *s* band at the bottom of the conduction band, (2) separation of this band from the valence band by a fundamental bandgap large enough to exclude interband transitions in the visible range, and (3) band properties such that the plasma frequency is below the visible range. In fact, the first condition provides the high mobility of the extra carriers introduced by the dopant, a pronounced B-M shift, which helps to keep intense interband transitions originating from the valence band out of the optical range (provided that the fundamental bandgap is big enough) and a relatively low intensity of interband transitions from the partially occupied band at the top of the conduction band. We note also that splitting of the highly dispersed band with doping helps to satisfy requirement (3) and also reduces contributions of the interband transitions. Thus, features of the band structure indicated in conditions (1) and (2) are the most important in selecting candidates and developing doping strategies for new TCOs.

Thin Films of Transparent Conducting Oxides

The principal application of TCOs is in the form of thin films, and a fundamental understanding of growth process–microstructure–charge transport–transparency relationships is crucial to designing new and improved materials. Notably, while bulk phase diagrams and crystal structures are essential foundations, they may not always reflect the rich range of metastable phases and solid solutions possible in thin films. This fascinating interplay between bulk and thin-film phenomena is motivating a closely interfaced film growth and characterization effort by two complementary techniques: metalorganic chemical vapor deposition (MOCVD) and pulsed laser deposition (PLD). The former process offers the attraction of *in situ* growth under a variety of atmospheres, amenability to large-area coverage with high throughput, conformal coverage, ready control of growth chemistry, the possibility of creating metastable structures, and the growth of multilayers in the pulsed mode. The latter technique offers the opportunity to conveniently grow films and multilayers of almost any composition for rapid exploratory scouting.

A key requirement for viable MOCVD processes is the availability of high-purity, thermally stable, volatile, and preferably low-melting metalorganic precursors having appropriate reactivity patterns to achieve efficient transport of the respective metal sources for clean film growth. Building on results from previous oxide growth studies,[26–29] known and new families of multidentate ligands that saturate the metal coordination sphere have been implemented in precursor synthesis and MOCVD growth of TCO films. Figure 4 illustrates several families of precursors that have been studied at Northwestern.[30–33]

In concert with the bulk materials studies mentioned earlier, the growth by low-pressure MOCVD and characterization of extensive series of Zn-In-O and Ga-In-O films[1,2] have been carried out with and without Sn donor-doping (Equation 3) and H_2 annealing (see Equations 4 and 5).[30–32] The microstructure, composition, and morphology of the MOCVD-derived TCO films have been scrutinized by x-ray

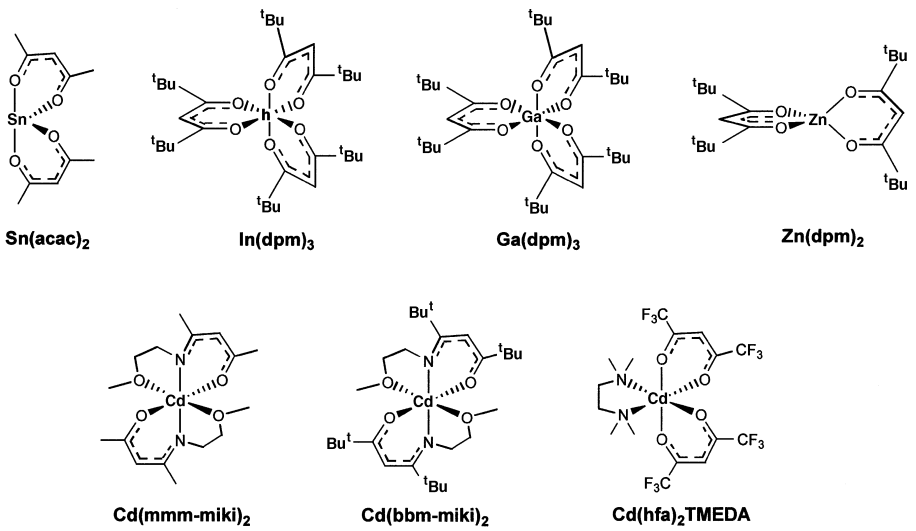

Figure 4. Metalorganic molecular precursors employed in the metalorganic chemical vapor deposition growth (MOCVD) of TCO films.

diffraction, high-resolution transmission electron microscopy, microdiffraction, atomic-resolution *Z*-contrast electron microscopy, high-resolution energy-dispersive x-ray analysis, and atomic force microscopy. Several trends are evident. For the Zn-In-O system, we find that films exhibit maximum 25°C conductivity (*n*-type, 1030 S/cm, $n = 4.5 \times 10^{20}$ cm^{-3}, $\mu =$ 14.3 cm^2/V s; Table III) at Zn/In ~ 0.33. The charge transport is metal-like ($d\sigma/dT < 0$), similar to that in Figure 5a, while the optical transparency is significantly greater than that of typical ITO films and the transparency window is broader, as shown in Figure 5b.[30] Microstructurally, we find that as-grown Zn-In-O films are polycrystalline, with diffraction features assignable to cubic Zn-doped In_2O_3 at low Zn levels and to ZnO at high Zn levels. At intermediate Zn incorporation levels, films consist of the layered $(ZnO)_kIn_2O_3$ phases[9,10] identified in the bulk studies mentioned previously, precipitated within a cubic In_2O_3:Zn matrix.[30] Annealing of these films under air is accompanied by a drastic decrease in conductivity and crystallization of a polytypoid structure having ZnO slabs of variable thickness separated by single octahedrally coordinated In-O layers.[34] Annealing these films under H_2 results in markedly increased electron mobility and carrier density with $\sigma(25°C) = 2700$ S/cm (Table III), with little detectable change in microstructure.

MOCVD growth of Zn-In-O films in the presence of a Sn-organic precursor yields films with Sn/(Zn + In) ratios in the range 0.0–2.2.[32,33,35,36] X-ray diffraction reveals poorly crystalline microstructures with broad reflections assignable to a cubic doped In_2O_3 structure. The maximum 25°C conductivity is found in films with the nominal composition $Zn_{2.0}In_{4.0}Sn_{3.0}O_{14}$ ($\sigma \sim 2300$ S/cm), as shown in Table III, reflecting considerable enhancement in the mobility but not in the electron density due to Sn doping. These Sn doping levels

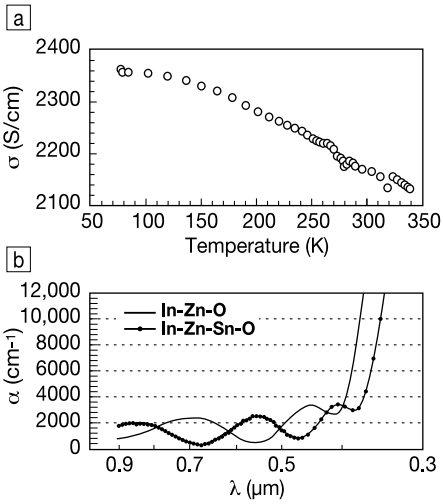

Figure 5. (a) Variable-temperature conductivity data for a $Zn_{2.0}In_{4.0}Sn_{3.0}$ film and (b) optical-transmission spectra of $Zn_{0.66}In_{2.0}O_{2.66}$ and $Zn_{2.0}In_{4.0}Sn_{3.0}O_{14}$ films.

effect little change in the film microstructure. The charge transport of these films is again metal-like (Figure 5a), and the optical transparency window is broader than those of ITO films and Sn-free Zn-In-O films (Figure 5b). This increase in the apparent bandgap upon doping may be attributable to a Burstein-Moss shift,[37,38] but may also reflect changes in the band structure (e.g., see Figure 3).[24] Interestingly, H_2 annealing of these films drastically reduces the carrier concentration, while leaving the mobility and microstructure essentially unchanged (Table III).

Ga-In-O films with Ga/(In + Ga) ratios of 0–0.55 and Ga-In-Sn-O films over a range of stoichiometries have also been grown by low-pressure MOCVD. Microstructural analysis of the Ga-In-O films indicates a cubic, homogeneously Ga-doped In_2O_3 structure.[32,33,35] Plan-view and cross-section transmission electron microscopy (TEM) analyses of Ga-In-Sn-O films reveal polycrystalline, cubic microstructures with grain size varying with exact growth conditions (Figure 6). The most conductive Ga-In-O compositions are in the region Ga/(Ga + In) ~ 0.05–0.07, with weakly metallic *n*-type charge transport, low carrier densities, and high mobilities (Table III). Upon reductive annealing, carrier concentration increases significantly, conductivity is clearly metallic (similar to that of Figure 7a), and the mobility, ~65 cm^2/V s, is one of the largest reported to date for a transparent conductor.[33] Compared to typical ITO films, the optical transparency windows of the Ga-In-O films are significantly broader (Figure 7b). Sn doping greatly increases the conductivity of the Ga-In-O films. Those with Ga/(In + Ga) ~ 0.05–0.06 and Sn/(In + Ga) ~ 0.5 exhibit the highest room-temperature conductivity, $\sigma \sim 3300$ S/cm, and pronounced metallic character (Figure 7a).[33,35,39,40] The optical transparency window again exceeds that of ITO films (Figure 7b). As in the Zn-In-Sn-O system, subsequent H_2 reductive annealing diminishes the carrier concentration while leaving the mobility unchanged (Table III).

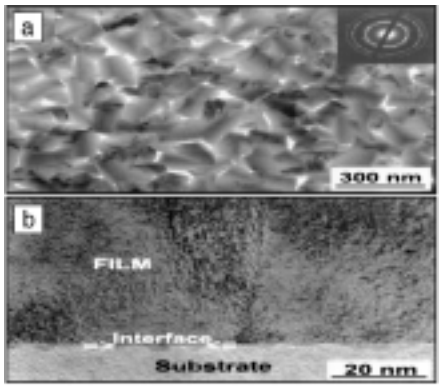

Figure 6. (a) Plan-view image and (b) cross-section transmission electron microscopy image of an $In_{30}Ga_{1.5}Sn_{15}O_x$ film.

Table III: Charge-Transport Characteristics of MOCVD-Derived TCO Films (at 25°C) Before and After Annealing.

Composition	$Zn_{0.66}In_2O_{2.66}$		$Zn_{2.0}In_{4.0}Sn_{3.0}O_{14}$		$In_{1.88}Ga_{0.12}O_3$		$In_{30}Ga_{1.5}Sn_{15}O_x$	
Processing	As-grown	Reductively annealed	As-grown	Reductively annealed	As-grown	Reductively annealed	As-grown	Reductively annealed
Carrier concentration *n* (10^{20} cm^{-3})	4.5	8.3	4.3	2.7	0.8	1.4	8.6	6.8
Mobility μ (cm^2/V s)	14.3	20.3	33.2	31.0	55.2	64.6	23.9	24.6
Conductivity σ (S/cm)	1030.0	2700.0	2290.0	1340.0	700.0	1400.0	3280.0	2680.0

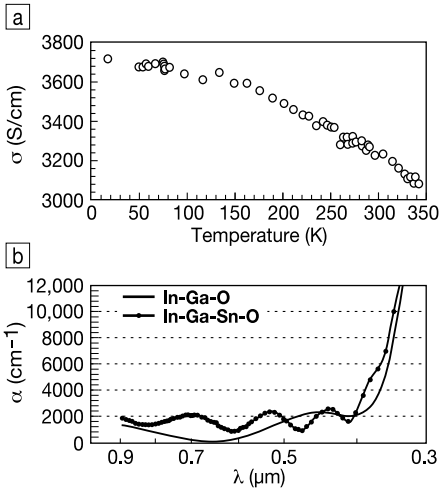

Figure 7. (a) Variable-temperature conductivity data for an $In_{30}Ga_{1.5}Sn_{15}O_x$ film, and (b) optical-transmission spectra of $In_{1.88}Ga_{0.12}O_{3.0}$ and $In_{30}Ga_{1.5}Sn_{15}O_x$ films.

Our group's film-growth effort has also focused on Cd-containing TCO phases. Thus a combinatoric study of the (Cd-In-Sn)-O system is being carried out by PLD. The phase diagram can be rapidly explored by creating multilayers of single oxides, with stoichiometry controlled by adjusting layer thickness. As-grown films with Cd:In:Sn stoichiometries of 2:0:1 (Cd_2SnO_4), 1:2:0 ($CdIn_2O_4$), and 1.7:0.6:0.7 exhibit 25°C conductivities ~1500–2300 S/cm in each case. Upon oxygen annealing, single-phase polycrystalline phases are readily formed; however, the carrier densities are significantly diminished for both Cd_2SnO_4 and $CdIn_2O_4$, but can be restored by reductive annealing in Ar. In contrast, the carrier density of the ternary cation composition is relatively insensitive to annealing, implicating one of the extrinsic carrier-generation mechanisms in Table II. The Cd-In-O and ternary oxide films exhibit mobilities in the range of 20–25 cm^2/V s, while the Cd-Sn-O films have a mobility of 33 cm^2/V s in the reduced state. The ternary oxide films exhibit ~80% transparency from 400 nm to 700 nm. These early films are far from optimized with respect to composition and microstructure; however, their behavior suggests further improvement can be anticipated by control of deposition–microstructure–property relationships.

MOCVD studies of Cd-based TCOs focused first on synthesizing a thermally stable, volatile Cd precursor more easily handled than $Cd(CH_3)_2$ and not providing a source of contaminating C. CdO growth[41,42] using $Cd(hfa)_2TMEDA$ (Figure 4)[41] yields *n*-type films with $\sigma(25°C) \sim 3500$ S/cm and $\mu \sim 200$ cm^2/V s. Remarkably, low levels of In doping (In/(In + Cd) ≤ 12 %) yield MOCVD-derived films with $\sigma(25°C)$ as high as 16,000 S/cm (5% doping level), metal-like charge transport, and a useful visible transparency window that broadens further upon In doping (Figure 8).[41,42] The microstructures of the most conductive In-Cd-O phases are CdO-like, as judged by x-ray diffraction and electron microscopy.

As an example of the present advanced state of the theory, we show in Figure 9 the band structure of CdO along high-symmetry directions in the Brillouin zone, determined by the self-consistent screened-exchange local-density approximation (SX-LDA) method, which successfully overcomes the shortcomings of LDA in treating excitations (such as bandgaps and band offsets). Strikingly, the calculated indirect and direct bandgaps, 2.86 eV and 0.63 eV, respectively, are in excellent agreement with experimental results.[42]

Conclusions and Prospects

Our work on bulk and thin-film phases in the (Zn-Cd-In-Ga-Sn)-O quintinary oxide system suggests that additional new, instructive, and useful compounds and solid-solution phases remain to be discovered and characterized for TCO properties. Many of these exhibit compositionally tailorable electrical/optical properties; that is, the potential exists for "engineered" transparent conducting oxides for a wide range of applications. Transparent conductors appear to share

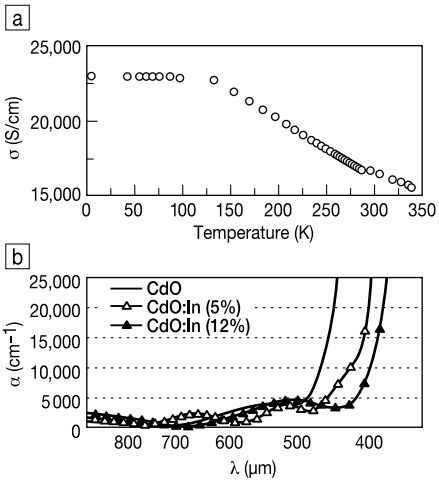

Figure 8. (a) Variable-temperature charge transport data for an $In_{0.50}Cd_{0.95}O$ film and (b) optical-transmission spectra for $In_xCd_{1.0-x}O$ films with the indicated In doping levels.

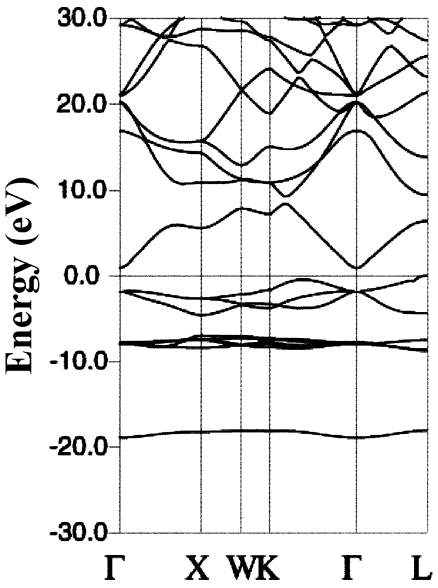

Figure 9. Band structure of CdO along high-symmetry directions in the Brillouin zone determined by the self-consistent screened-exchange local-density approximation method.[25]

common structural features (for instance, In and/or a combination of Cd and Sn on octahedral sites) and similar carrier-generation mechanisms by means of aliovalent doping and/or reduction. First-principles electronic structure theory is an important tool for understanding structure–composition–property relationships in these new materials.

Our film work demonstrates that with the appropriate metalorganic precursors, MOCVD is a viable means to grow a large variety of high-quality TCO films. Structural systematics in the Zn-In-O and Ga-In-O series of MOCVD-derived films, before and after Sn or reductive doping, are at this stage considerably more complex and less resolved than in the corresponding bulk materials. This doubtless reflects an interplay of several factors, including film-structure formation far from equilibrium, due both to the kinetics of the growth processes and the temperatures of nucleation and growth. Nevertheless, doping by incorporation of Sn or annealing under H_2 are remarkably effective in both enhancing charge transport and in widening the optical transparency window, for reasons that are best understood only qualitatively at this time. The Cd-In-O and In-Cd-Sn-O film systems are even less explored; however, the high conductivities and mobilities are especially intriguing. In general, these TCO films are far less crystalline and ordered than the bulk materials, and most attempts to induce

greater crystallinity are usually accompanied by loss of conductivity. However, it is intriguing and worthy of additional investigation that doped cubic In_2O_3 or CdO phases are ubiquitous in the most conductive of the film microstructures.

Considerable potential exists for the discovery and development of new complex oxides with enhanced TCO properties within (Zn-Cd-In-Ga-Sn)-O phase space. A combinatoric exploratory approach to bulk and thin films, combining theory and experimentation, is essential to fully understand and optimize these important new materials.

Acknowledgments

This work was supported in part by the NSF-MRSEC program (grant No. DMR-9632472) and in part by the U.S. Department of Energy through the National Renewable Energy Laboratory (subcontract No. AAD-9-18668-05). A number of current and former students, staff, and colleagues participated in this effort, including C.R. Kannewurf, T. Moriga, D.D. Edwards, G.B. Palmer, O.N. Mryasov, R. Asahi, X.Y. Huang, K.-T. Park, A. Ambrosini, D. Ko, M. Yan, A. Wang, N.L. Edleman, J.R. Babcock, A.W. Metz, M.V. Metz, and D.R. Kammler.

References

1. R.J. Cava, J.M. Phillips, J. Kwo, G.A. Thomas, R.B. van Dover, S.A. Carter, J.J. Krajewski, W.F. Peck, Jr., J.H. Marshall, and D.H. Rapkine, *Appl. Phys. Lett.* **64** (1994) p. 2071.
2. J.M. Phillips, R.J. Cava, G.A. Thomas, S.A. Carter, J. Kwo, T. Siegrist, J.J. Krajewski, J.H. Marshall, W.F. Peck Jr., and D.H. Rapkine, *Appl. Phys. Lett.* **67** (1995) p. 2246.
3. D.D. Edwards, "Phase Relations, Crystal Structures, and Electrical Properties of Select Oxides in the Gallium-Indium-Tin-Oxide System," PhD thesis, Northwestern University, 1997.
4. G.B. Palmer, "Phase Relations and Physical Properties of New Transparent Conductors in the (Indium, Gallium)-Tin-Zinc Oxide Systems," PhD thesis, Northwestern University, 1999.
5. T. Moriga, D.R. Kammler, T.O. Mason, G.B. Palmer, and K.R. Poeppelmeier, *J. Am. Ceram. Soc.* **82** (1999) p. 2705.
6. D.R. Kammler (unpublished manuscript).
7. D.D. Edwards, T.O. Mason, F. Goutenoire, and K.R. Poeppelmeier, *Appl. Phys. Lett.* **70** (1997) p. 1706.
8. D.D. Edwards, T.O. Mason, W. Sinkler, L.D. Marks, F. Goutenoire, and K.R. Poeppelmeier, *J. Solid State Chem.* **140** (1998) p. 242.
9. M. Nakamura, N. Kimizuka, and T. Mohri, *J. Solid State Chem.* **93** (1991) p. 298.
10. T. Moriga, D.D. Edwards, T.O. Mason, G.B. Palmer, K.R. Poeppelmeier, J.L. Schindler, C.R. Kannewurf, and I. Nakabayashi, *J. Am. Ceram. Soc.* **81** (1998) p. 1310.
11. C. Li, Y. Bando, M. Nakamura, and N. Kimizuka, *Jpn. Soc. Electron Microsc.* **46** (1997) p. 119.
12. G.B. Palmer, K.R. Poeppelmeier, and T.O. Mason, *Chem. Mater.* **9** (1997) p. 3121.
13. D.R. Kammler, T.O. Mason, and K.R. Poeppelmeier, *Chem. Mater.* (2000) in press.
14. R.D. Shannon, J.L. Gillson, and R.J. Bouchard, *J. Phys. Chem. Solids* **38** (1977) p. 877.
15. G.B. Palmer, K.R. Poeppelmeier, and T.O. Mason, *J. Solid State Chem.* **134** (1997) p. 192.
16. X. Wu, T.J. Coutts, and W.P. Mulligan, *J. Vac. Sci. Technol., A* **15** (1997) p. 1057.
17. C.M. Cardile, A.J. Koplick, R. McPherson, and B.O. West, *J. Mater. Sci. Lett.* **8** (1989) p. 370.
18. T. Stapinski, E. Japa, and J. Zukrowski, *Phys. Status Solidi A* **103** (1987) p. K93.
19. G. Frank and H. Kostlin, *Appl. Phys. A* **27** (1982) p. 197.
20. J.-H. Hwang, D.D. Edwards, D.R. Kammler, and T.O. Mason, *Solid State Ionics* **129** (2000) p. 135.
21. G. Gonzalez, J. Cohen, J.-H. Hwang, T. Mason, J. Hodges, and J. Jorgensen, "Defect Structures of Indium Tin Oxide and Its Relationship to Conductivity," in *Proc. Int. Conf. Mass and Charge Transport in Inorganic Materials*, edited by P. Vincenzini (Techna Publishers, Faenza, Italy, 2000) in press.
22. R. Dieckmann and H. Schmalzried, *Phys. Chem.* **81** (1977) p. 414.
23. G. Haacke, W.E. Mealmaker, and L.A. Siegel, *Thin Solid Films* **55** (1978) p. 67.
24. O.N. Mryasov and A.J. Freeman, *Phys. Rev. B* (submitted for publication).
25. X.Y. Huang, R. Asahi, K.-T. Park, and A.J. Freeman (unpublished manuscript).
26. J.A. Belot, R.J. McNeely, A. Wang, C.J. Reedy, T.J. Marks, G.P.A. Yap, and A.L. Rheingold, *J. Mater. Res.* **14** (1999) p. 15.
27. J.A. Belot, A. Wang, R.J. McNeely, L. Liable-Sands, A.L. Rheingold, and T.J. Marks, *Chem. Vap. Depos.* **5** (1999) p. 65.
28. D.A. Neumayer, J.A. Belot, R.L. Feezel, C.J. Reedy, C.L. Stern, T.J. Marks, L.M. Liable-Sands, and A.L. Rheingold, *Inorg. Chem.* **37** (1998) p. 5625.
29. J.A. Belot, D.A. Neumayer, C.J. Reedy, D.B. Studebaker, B.J. Hinds, C.L. Stern, and T.J. Marks, *Chem. Mater.* **9** (1997) p. 1638.
30. A. Wang, S.C. Cheng, M.P. Chudzik, T.J. Marks, R.P.H. Chang, and C.R. Kannewurf, *Appl. Phys. Lett.* **73** (1998) p. 327.
31. A. Wang, S.C. Cheng, J.A. Belot, R.J. McNeely, J. Cheng, B. Marcordes, T.J. Marks, J.Y. Dai, R.P.H. Chang, J.L. Schindler, M.P. Chudzik, and C.R. Kannewurf, in *Chemical Aspects of Electronic Ceramics Processing*, edited by P.N. Kumta, A.F. Hepp, D.B. Beach, B. Arkles, and J.J. Sullivan (Mater. Res. Soc. Symp. Proc. **495**, Warrendale, PA, 1998) p. 3.
32. A. Wang, N.L. Edleman, J.R. Babcock, T.J. Marks, M.A. Lane, P.W. Brazis, and C.R. Kannewurf, Mater. Res. Soc. Symp. Series in press.
33. J.R. Babcock, N.L. Edleman, A. Wang, C.L. Stern, and T.J. Marks, *Adv. Mater. CVD* (2000) in press.
34. Y. Yan, S.J. Pennycook, J. Dai, R.P.H. Chang, A. Wang, and T.J. Marks, *Appl. Phys. Lett.* **73** (1998) p. 2585.
35. A. Wang, N.L. Edleman, T.J. Marks, M.A. Lane, P.W. Brazis, and C.R. Kannewurf, submitted for publication.
36. T. Minami, T. Kakumu, K. Shimokawa, and S. Takata, *Thin Solid Films* **317** (1–2) (1998) p. 318.
37. B.E. Sernelius, K.-F. Berggren, Z.-C. Jin, I. Hamberg, and C.G. Granqvist, *Phys. Rev. B* **37** (1988) p. 244.
38. E. Burstein, *Phys. Rev.* **93** (1954) p. 632.
39. T. Minami, T. Kakumu, and S. Takata, *J. Vac. Sci. Technol., A* **14** (1996) p. 1704.
40. T. Minami, Y. Takeda, T. Kakumu, S. Takata, and I. Fukuda, *J. Vac. Sci. Technol., A* **15** (1997) p. 958.
41. J.R. Babcock, A. Wang, N.L. Edleman, D.D. Benson, A.W. Metz, M.V. Metz, and T.J. Marks, "Development and Implementation of New Volatile Cd and Zn Precursors for the Growth of Transparent Conducting Oxide Thin Films via MOCVD," presented at the Spring 2000 Materials Research Society Meeting, San Francisco, CA, April 27, 2000.
42. A. Wang, J.R. Babcock, N.L. Edleman, M.A. Lane, S. Yang, C.R. Kannewurf, A.J. Freeman, and T.J. Marks (manuscript in preparation). □